Coherence-mediated squeezing of a cavity field coupled to a coherently driven single quantum dot

Parvendra Kumar [1,2,*] and Agnikumar G. Vedeshwar [1,†]

[1]*Department of Physics and Astrophysics, Thin Film Laboratory, University of Delhi, Delhi 110007, India*

[2]*Department of Physics, Bhagini Nivedita College, University of Delhi, New Delhi 110043, India*

(Received 9 July 2021; accepted 14 February 2022; published 17 March 2022)

Coherence has been an important key for numerous applications of quantum physics ranging from quantum metrology to quantum information. We report here a theoretical paper demonstrating how maximally created coherence results in the squeezing of a cavity field coupled to a coherently driven single quantum dot. We employ a polaron master equation theory for accurately incorporating the impact of exciton-phonon coupling on squeezing.

DOI: 10.1103/PhysRevA.105.033710

I. INTRODUCTION

Quantum coherence is an important ubiquitous feature of quantum physics that results from the superposition of constituent states of the quantum system. It has been exploited extensively and serves as an important resource in many diverse fields, such as quantum information and quantum computing [1–3], quantum metrology [4–6], quantum biology [7,8], and quantum transport [9,10]. Furthermore, the ability to create and control the coherence is a key requirement for the realization of several practically important concepts, such as coherent population trapping and electromagnetically induced transparency [11–16], steady-state population inversion [17], and lasing without inversion [18]. Recently, coherence is also shown to facilitate the squeezing of the resonance fluorescence of a two-level atom [19]. It is to be noted that this approach is quite different from the usual approach based on nonlinear processes in variety of systems, such as the Kerr effect, multiwave mixing in atomic, solid-state systems [20–23], cavity quantum electrodynamics, cavity optomechanics [24–26], and Bose-Einstein condensation [27]. Here, it is quite worthwhile to mention that the squeezing that refers to a noise reduction below the shot noise in either of the quadratures at an expense of increased noise in a canonically conjugate quadrature. Therefore, squeezing is found to be quite useful for various applications in quantum metrology and gravitational wave detection [28–31].

Recently, there has been great interest in utilizing the solid-state systems, such as quantum dots, superconducting circuits, and nitrogen-vacancy centers in diamond for the generation of quantum light, viz. single photons, entangled photon pairs [32–35], and squeezed light [36]. In particular, the squeezing of the resonance fluorescence (RF) of an isolated single quantum dot (QD) in free space has been demonstrated very recently [37–39]. However, for practical applications, squeezing of the cavity mode field seems to be more useful and desirable too. This is particularly due to the fact that the photons emitted through the cavity mode can be extracted much efficiently through an optical fiber or a waveguide as compared to the photons emitted through the free space modes. In this paper, we theoretically demonstrate the squeezing of the cavity field strongly coupled to a coherently driven single QD. First, we investigate the optimum values of parameters of a QD-cavity system such as Rabi frequency, detunings, cavity coupling strength, and cavity decay rate for obtaining the maximal squeezing of the cavity field. We show that the squeezing of cavity field depends upon the exciton coherence which couples back to the cavity mode via a two-photon state. We further show that the buildup of maximal exciton coherence causes the creation of coherence between the Fock states of the cavity mode enabling the emergence of the squeezing effect. Since the exciton state of a quantum dot unavoidably interacts with the phonon modes, we also analyze the effect of the temperature-dependent exciton-phonon coupling on the squeezing of cavity field by employing a polaron master equation theory. It may be necessary to clarify here that in Refs. [19,40], the optimal squeezing of RF of a two-level emitter coupled to a cavity was demonstrated only in the weak-coupling regime, whereas in the present paper we show that the optimal squeezing of cavity field can be obtained in a strongly coupled QD-cavity system in sharp contrast with the earlier works. Furthermore, the squeezing of RF was shown to depend only on the exciton coherence by earlier works, whereas we show that the squeezing of the cavity field depends on both the exciton coherence and the two-photon process.

II. THEORETICAL FORMALISM

A. Model of the dot-cavity system

We consider a single self-assembled InGaAs/GaAs QD strongly coupled to a single-mode pillar microcavity. The QD is modeled as a two-level system considering its ground and exciton states represented by $|g\rangle$ and $|e\rangle$, respectively. A schematic of the relevant Jaynes-Cummings

*parvendra1986@gmail.com

†agni@physics.du.ac.in

 ©2022 American Physical Society

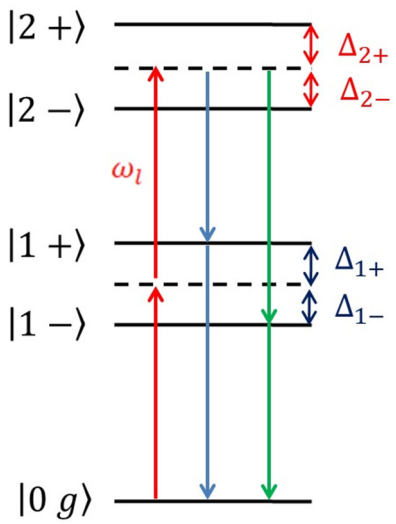

FIG. 1. Schematic of a single QD strongly coupled to a mode of an optical cavity in the Jaynes-Cummings basis. The QD is excited by a continuous wave (cw) laser light of frequency of ω_l. Two laser photons are absorbed (red arrows) and reemitted (blue and green arrows).

basis states ladder of a QD-cavity system is shown in Fig. 1. Denoting the cavity photon states $|n\rangle$ with $n = 0–2, \ldots,$ the Jaynes-Cummings basis states are given by $|0\ g\rangle = |0\rangle|g\rangle$, $|1\pm\rangle = 1/\sqrt{2}(|1\rangle|g\rangle \pm |0\rangle|e\rangle)$, and $|2\pm\rangle = 1/\sqrt{2}(|2\rangle|g\rangle \pm |1\rangle|e\rangle)$. The $\Delta_{n\pm} = \omega_l - \omega_{n\pm}$ is the detuning of laser light with respect to the frequencies of the dressed states $|n\pm\rangle$ [24]. We consider that the QD is excited by a cw laser light of frequency of ω_l. Two photons are absorbed from the laser light (red arrows) and reemitted via the path shown by blue and green arrows. The two-photon processes together with the exciton coherence leads to the squeezing of the cavity field as described in the next section.

B. Effective polaron master equation theory

In contrast to the real atoms, the exciton states of QDs are unavoidably coupled to their phonon modes. For a typical coherently driven InGaAs/GaAs QDs, the coupling of longitudinal acoustic phonon bath is found to be quite dominant and influential as compared to the optical-phonon bath, leading to the excitation-induced incoherent scattering and dephasing of exciton and biexciton states of QDs [41,42]. Several theoretical methods, such as path integral, the variational method, and polaron transformation are utilized for accurately incorporating the effect of exciton-phonon coupling depending upon the various concerned parameters, such as Rabi frequency, cavity coupling strength, and temperature of the phonon bath [43–45]. In this paper, we chose to employ a polaron transformation-based equation, the so-called effective polaron master equation (EPME). Under the suitable parameter regime, this equation is quite known for providing the accurate results, much faster computation, and deeper understanding of the phonon-mediated processes through the analytical form of phonon-induced incoherent scattering rates. It is worthwhile to mention here that the EPME gives the accurate results in the regime of Ω^{-1} and g_c^{-1} being much larger than the phonon correlation time ($\tau_{\rm ph} \approx 2$ ps) or when the detunings ($\Delta_{\rm xl}$, $\Delta_{\rm cx}$) are much larger than the Rabi frequency Ω and QD-cavity coupling strength g_c [46]. The EPME for our QD-cavity system shown in Fig. 1 is given below. The procedural details for deriving the EPME can be found in Refs. [45–47],

$$\frac{d\rho(t)}{dt} = -\frac{i}{\hbar}[H_s,\ \rho(t)] + \frac{\Gamma_{\rm ph}^{\sigma^+}}{2}L[\sigma^+]\rho(t) + \frac{\Gamma_{\rm ph}^{\sigma^-}}{2}L[\sigma^-]\rho(t) + \frac{\Gamma_{\rm ph}^{a^\dagger\sigma^-}}{2}L[a^\dagger\sigma^-]\rho(t) + \frac{\Gamma_{\rm ph}^{\sigma^+ a}}{2}L[\sigma^+ a]\rho(t) + L[\rho(t)], \tag{1}$$

The Hamiltonian of the QD-cavity system reads as

$$H_s = \hbar\Delta_{\rm xl}\sigma^+\sigma^- + \hbar\Delta_{\rm cl}a^\dagger a + \langle B\rangle\hbar\left[\frac{\Omega}{2}(\sigma^+ + \sigma^-) + g_c(\sigma^+ a + a^\dagger\sigma^-)\right], \tag{2}$$

where $\Delta_{\rm xl} = \omega_x - \omega_l$ is the detuning of the cw laser field with respect to exciton state, whereas $\Delta_{\rm cl} = \omega_c - \omega_l$ is the detuning of laser field with respect to cavity mode. The operators $\sigma^+ = |e\rangle\langle g|$ and $\sigma^- = |e\rangle\langle g|$ are the raising and lowering operators, and $a^\dagger$ and a are the one-photon creation and annihilation operators. The thermally averaged phonon displacement operator $\langle B\rangle$ is defined as $\langle B\rangle = \exp[-\frac{1}{2}\int_0^\infty d\omega\frac{J(\omega)}{\omega^2}\coth(\frac{\hbar\omega}{2K_BT})]$, where T represents the temperature of the phonon bath. The phonon spectral function $j(\omega)$ quantifies the exciton-phonon coupling and is defined as $j(\omega) = \alpha_P\omega^3\exp(-\frac{\omega^2}{2\omega_b^2})$. Here α_P represents the strength of exciton-phonon coupling, and ω_b represents the cutoff frequency of the phonon bath. The Rabi frequency is defined as $\Omega = \mu E/\hbar$, where μ and E represent the exciton electric dipole moment and electric field of the cw laser, respectively. The operators $\Gamma_{\rm ph}^{\sigma^+}$ and $\Gamma_{\rm ph}^{\sigma^-}$ represent the phonon-induced incoherent excitation and deexcitation rates of the exciton state, whereas $\Gamma_{\rm ph}^{a^\dagger\sigma^-}$ and $\Gamma_{\rm ph}^{\sigma^+ a}$ represent the rates of phonon-induced creation of the cavity photon accompanied by the decay of the exciton state and annihilation of the cavity photon accompanied by the excitation of the exciton state, respectively. These phonon-induced incoherent rates are given as

$$\Gamma_{\rm ph}^{\sigma^+/\sigma^-} = \frac{\Omega_R^2}{2}{\rm Re}\left[\int_0^\infty d\tau e^{\pm i\Delta_{\rm lx}\tau}(e^{\phi(\tau)} - 1)\right] \tag{3a}$$

$$\Gamma_{\rm ph}^{\sigma^+ a/a^\dagger\sigma^-} = 2g_R^2{\rm Re}\left[\int_0^\infty d\tau e^{\pm i\Delta_{\rm cx}\tau}(e^{\phi(\tau)} - 1)\right], \tag{3b}$$

where, $\Omega_R = \langle B\rangle\Omega$ and $g_R = \langle B\rangle g_c$ are the phonon-renormalized Rabi frequency and phonon-renormalized cavity coupling strength, respectively. The average phonon displacement operator $\langle B\rangle$ is 0.91 at $T = 4$ K. The term $\phi(\tau)$ represents the phonon phase, which is given as $\phi(\tau) = \int_0^\infty d\omega\frac{j(\omega)}{\omega^2}[\coth(\frac{\hbar\omega}{2K_BT})\cos(\omega\tau) - i\sin(\omega\tau)]$ in the continuum limit. The last term $L[\rho(t)]$ in Eq. (1) is added phenomenologically for incorporating the natural radiative decay γ pure dephasing γ' rates of exciton state along with the cavity decay rate κ. It reads as $L[\rho(t)] = \frac{\gamma}{2}L[\sigma^-]\rho(t) + \frac{\gamma'}{2}L[\sigma^+\sigma^-]\rho(t) + \frac{\kappa}{2}L[a]\rho(t)$.

III. NUMERICAL RESULTS AND DISCUSSIONS

We investigate the squeezing of the cavity field by analyzing the variance of the quadratures $X_\theta = \frac{1}{2}(a^\dagger e^{i\theta} + a e^{-i\theta})$, where θ is an adjustable phase. Furthermore, we define the variance and fluctuation of a with respect to the steady-state value $\langle a\rangle$ as $\langle \Delta X_\theta^2\rangle = \langle (X_\theta - \langle X_\theta\rangle)^2\rangle$ and $\Delta a = a - \langle a\rangle$, respectively. The normally ordered quadrature variance for $\theta = 0$ is given by $\langle : \Delta X^2 : \rangle = \frac{1}{2}[\langle \Delta a\, \Delta a^\dagger\rangle + \mathrm{Re}(\Delta a^2)]$. For a vacuum or coherent state, $\langle \Delta a\, \Delta a^\dagger\rangle = \Delta a^2 = 0$. Thus, the normally ordered variance is equal to the shot noise, that is $\langle : \Delta X^2 : \rangle = 0$. Therefore, the state of the cavity field will be quadrature squeezed if the normally ordered variance becomes negative, $\langle : \Delta X^2 : \rangle < 0$, corresponding to a noise reduction below vacuum level. The normally ordered variance in terms of the expectation values of cavity operators is as follows:

$$\langle : \Delta X^2 : \rangle = \tfrac{1}{2}[\langle a^\dagger a\rangle - \langle a\rangle\langle a^\dagger\rangle + \mathrm{Re}\big(\langle a^2\rangle - \langle a\rangle^2\big)]. \quad (4)$$

The squeezing of cavity field is investigated by numerically solving Eq. (1) for calculating the expectation values of involved operators in Eq. (4), via $\langle O\rangle = \mathrm{Tr}(O\rho)$, where O is an arbitrary operator. The term $\langle \Delta a\, \Delta a^\dagger\rangle = \langle a^\dagger a\rangle - \langle a\rangle\langle a^\dagger\rangle$ is the incoherent part of the spectrum and, hence, can never be negative. Therefore, this term should be as small as possible in order to observe the squeezing, which can be achieved for low enough excitation Rabi frequency or for a sufficiently large detuning, $\Delta_{\mathrm{xl}} \gg \Omega_R$ [24,46]. In the limit of large detuning, the incoherent part becomes negligible compared to the coherent part $\mathrm{Re}(\langle a^2\rangle - \langle a\rangle^2) = \mathrm{Re}(\Delta a^2)$ and the normally ordered variance reduces to

$$\langle : \Delta X^2 : \rangle \approx \tfrac{1}{2}[\mathrm{Re}(\Delta a^2)]. \quad (5)$$

We investigate the origin of squeezing using an approximate analytical expression of the normally ordered variance [see the Appendix] given by

$$\langle : \Delta X^2 : \rangle \approx -\frac{1}{2}\mathrm{Re}(K\langle\sigma^-\rangle^2), \quad (6)$$

$$\langle a\rangle = \frac{g_R}{\tilde{\omega}_c}\langle\sigma^-\rangle, \quad (7)$$

$$\langle a^2\rangle = \frac{\Omega_R}{\tilde{\omega}_c}K\langle\sigma^-\rangle, \quad (8)$$

where $\langle\sigma^-\rangle = \frac{\Omega_R\tilde{\omega}_c}{2(\tilde{\omega}_{1+}\tilde{\omega}_{1-})}$ is the exciton coherence, $K = \frac{2g_R^2}{(\tilde{\omega}_{2+}\tilde{\omega}_{2-})}$ is a constant and $\tilde{\omega}_{n\pm}$'s are the complex frequencies as defined in the Appendix. It is evident from Eq. (6) that the squeezing is directly depending on the exciton coherence and, hence, highlights its importance for achieving the maximal squeezing. Furthermore, the exciton coherence depends only on the one-photon excitation process as it is concerned only with one-photon dressed states $|1\pm\rangle$, whereas in contrast, the constant K affects the squeezing of the cavity field to the two-photon dressed states $|2\pm\rangle$ highlighting the importance of two-photon processes as depicted in Fig. 1.

In simulation, we use the typical values of QD parameters as $\gamma = 0.5\ \mu$eV, $\alpha_P/(2\pi)^2 = 0.06$ ps^2, $\gamma' = 1\ \mu$eV, and $\omega_b = 1$ meV [45,46]. The maximum values of the employed Rabi frequency, Ω, and cavity coupling strength g_c are chosen to be 109.89 and 164.83 μeV, respectively. It is to be noted that for these values, Ω^{-1} and g_c^{-1} turn out to be 38 and 25 ps, respectively, which are much greater than the phonon correlation time ($\tau_{\mathrm{ph}} \approx 2$ ps). Therefore, in this paper, the validity condition of EPME is clearly satisfied.

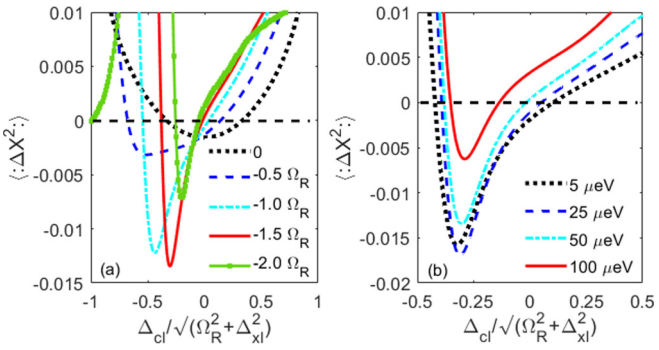

FIG. 2. (a) Evolution of the variance as a function of Δ_{cl} for five different values of detuning, $\Delta_{\mathrm{xl}} = 0$ (dotted black line), $\Delta_{\mathrm{xl}} = -0.5\Omega_R$ (dashed blue line), $\Delta_{\mathrm{xl}} = -1.0$ (dashed-dot cyan line), $\Delta_{\mathrm{xl}} = -1.5\Omega_R$ (solid red line), and $\Delta_{\mathrm{xl}} = -2.0\Omega_R$ (green square). (b) Evolution of the variance as a function of Δ_{cl} at $\Delta_{\mathrm{xl}} = -1.5\Omega_R$ for four different values of Rabi frequency, $\Omega_R = 5\ \mu$eV (dotted black line), $\Omega_R = 25\ \mu$eV (dashed blue line), $\Omega_R = 50\ \mu$eV (dashed-dot cyan line), and $\Omega_R = 100\ \mu$eV (solid red line). The values of the other parameters are taken as $\Omega_R = 50\ \mu$eV, $g_R = 1.5\Omega_R$, $\kappa = 0.9\Omega_R$, and $T = 4$ K. The horizontal dashed black line is a reference demarkation above which variance is positive and, hence, no squeezing.

A. Evolution of variance as a function of detuning and cavity coupling strength

We now investigate the optimum values of parameters of the QD-cavity system, such as detunings Δ_{cl}, Δ_{xl}, and Rabi frequency Ω_R for obtaining the maximal squeezing as depicted in Fig. 2. We show the evolution of the variance as a function of Δ_{cl} for a fixed value of $\Omega_R = 50\ \mu$eV and different values of Δ_{xl} in Fig. 2(a). It can be observed that the negative variance is maximum for $\Delta_{\mathrm{xl}} = -1.5\Omega_R$ at $\Delta_{\mathrm{cl}} = -0.3\sqrt{\Omega_R^2 + \Delta_{\mathrm{xl}}^2}$. We show the interdependence of various parameters of concern in Fig. 3 for understanding the squeezing better. We find that for $\Delta_{\mathrm{xl}} = -1.5\Omega_R$, the incoherent part $\langle a^\dagger a\rangle - \langle a\rangle\langle a^\dagger\rangle$ takes a minimum positive value together with maximal negative value of exciton coherence $\langle\sigma^-\rangle$ for $\Delta_{\mathrm{cl}} = -0.3\sqrt{\Omega_R^2 + \Delta_{\mathrm{xl}}^2}$ in comparison with the values of all other detunings as clearly evident from Fig 3. Therefore, $\langle a^2\rangle$ which depends on $\langle\sigma^-\rangle$ takes a larger negative value as compared to a smaller positive value of $-\langle a\rangle^2$ depending on $\langle\sigma^-\rangle^2$ [see Eqs. (7) and (8)]. Consequently, the negative variance and, hence, squeezing gets increased as clearly illustrated and further clarified in Fig. 3. Thus, with the chosen values of Ω_R, g_R, κ, $\Delta_{\mathrm{xl}} = -1.5\Omega_R$, and $\Delta_{\mathrm{cl}} = -0.3\sqrt{\Omega_R^2 + \Delta_{\mathrm{xl}}^2}$ are found to be the optimum for detunings. It should also be noted that the exactly same squeezing can be achieved for the same set of positive detunings Δ_{xl} and Δ_{cl}. We show the

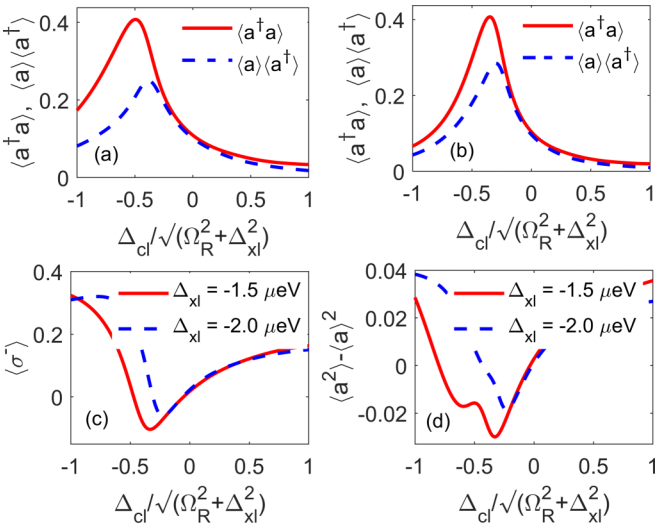

FIG. 3. Evolution of $\langle a^\dagger a\rangle$ (solid red line) and $\langle a\rangle\langle a^\dagger\rangle$ (dashed blue line) as a function of $\Delta_{\rm cl}$ for (a) $\Delta_{\rm xl} = -1.5\Omega_R$ and (b) $\Delta_{\rm xl} = -2.0\Omega_R$. Evolution of (c) coherence $\langle\sigma^-\rangle$ and (d) $\langle a^2\rangle - \langle a\rangle^2$ as a function of $\Delta_{\rm cl}$ for two different values of detuning, $\Delta_{\rm xl} = -1.5\Omega_R$ (solid red line) and $\Delta_{\rm xl} = -2.0\Omega_R$ (dashed blue line). The values of the other parameters are taken as $\Omega_R = 50\ \mu$eV, $g_R = 1.5\Omega_R$, $\kappa = 0.9\Omega_R$, and $T = 4$ K.

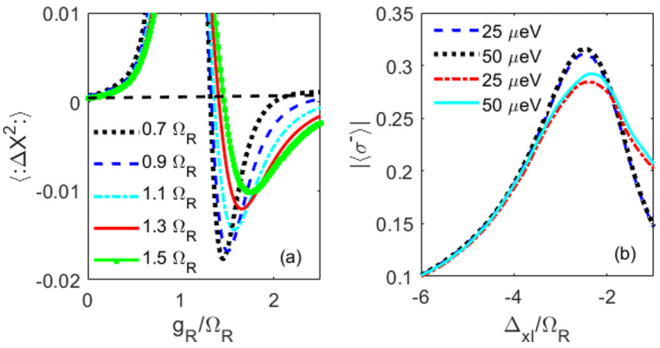

FIG. 4. (a) Evolution of the variance as a function of g_R for five different values of cavity decay rate, $\kappa = 0.7\Omega_R$ (dotted black line), $\kappa = 0.9\Omega_R$ (dashed blue line), $\kappa = 1.1\Omega_R$ (dashed-dot cyan line), $\kappa = 1.3\Omega_R$ (solid red line), and $\kappa = 1.5\Omega_R$ (green square). (b) Evolution of the coherence as a function of $\Delta_{\rm xl}$ without incorporating the exciton-phonon coupling for two different values of Rabi frequency, $\Omega_R = 25$ and 50 μeV (dashed blue and dotted black lines are numerically calculated, whereas dashed-dot red and solid cyan lines are analytically calculated). The values of other parameters are taken as $\Omega_R = 25\ \mu$eV, $\Delta_{\rm xl} = -1.5\Omega_R$, $\Delta_{\rm cl} = -0.3\sqrt{\Omega_R^2 + \Delta_{\rm xl}^2}$, and $T = 4$ K. The horizontal dashed black line is a reference demarkation above which variance is positive and, hence, no squeezing.

evolution of variance in Fig. 2(b) as a function of $\Delta_{\rm cl}$ for the various values of Ω_R for optimized $\Delta_{\rm xl} = -1.5\Omega_R$. It can clearly be observed that the negative variance is maximum for $\Omega_R = 25\ \mu$eV at $\Delta_{\rm cl} = -0.3\sqrt{\Omega_R^2 + \Delta_{\rm xl}^2}$. However, the negative variance decreases drastically for $\Omega_R = 50$ and 100 μeV. This can particularly be ascribed as due to the phonon-induced appreciable reduction in the exciton coherence with increasing Ω_R as explained in Sec. III B. Therefore, it is quite clear that $\Delta_{\rm xl} = -1.5\Omega_R$, $\Delta_{\rm cl} = -0.3\sqrt{\Omega_R^2 + \Delta_{\rm xl}^2}$, and $\Omega_R = 25\ \mu$eV are the optimum values for detunings and Rabi frequency, respectively.

Furthermore, the occurrence of a greater squeezing in Fig. 2(a) for $\Delta_{\rm xl} = -1.5\Omega_R$ for $\Delta_{\rm cl} = -0.3\sqrt{\Omega_R^2 + \Delta_{\rm xl}^2}$ can be more clearly demonstrated with reasoning through the evolution of various terms in Eq. (4) for the two different detunings. In Figs. 3(a) and 3(b), we show the evolution of $\langle a^\dagger a\rangle$ and $\langle a\rangle\langle a^\dagger\rangle$ as a function of $\Delta_{\rm cl}$ for the two different values of $\Delta_{\rm xl} = -1.5\Omega_R$ and $\Delta_{\rm xl} = -2.0\Omega_R$, respectively. It is clear that for both these detunings, the difference $[\langle a^\dagger a\rangle - \langle a\rangle\langle a^\dagger\rangle]$ never takes a negative value for any value of $\Delta_{\rm cl}$, however, it is minimum for $\Delta_{\rm cl} = -0.3\sqrt{\Omega_R^2 + \Delta_{\rm xl}^2}$, which is essential for obtaining the maximally negative variance [see Eq. (4)]. Next, we depict the evolution of exciton coherence $\langle\sigma^-\rangle$ as a function of $\Delta_{\rm cl}$ for $\Delta_{\rm xl} = -1.5\Omega_R$ and $\Delta_{\rm xl} = -2.0\Omega_R$ in Fig. 3(c). It is clear that $\langle\sigma^-\rangle$ takes a larger negative value for $\Delta_{\rm xl} = -1.5\Omega_R$ than $\Delta_{\rm xl} = -2.0\Omega_R$. Since $\langle a^2\rangle$ and $\langle a\rangle^2$ depend on $\langle\sigma^-\rangle$ and $\langle\sigma^-\rangle^2$, respectively, therefore, $\langle a^2\rangle - \langle a\rangle^2$ results in a larger negative value for $\Delta_{\rm xl} = -1.5\Omega_R$ than $\Delta_{\rm xl} = -2.0\Omega_R$ as shown in Fig. 3(d). All these together cause a larger squeezing for $\Delta_{\rm xl} = -1.5\Omega_R$ for $\Delta_{\rm cl} = -0.3\sqrt{\Omega_R^2 + \Delta_{\rm xl}^2}$. Next, we investigate the optimum values of g_R and κ with these optimized values.

We show in Fig. 4, the evolution of the variance and coherence as a function of g_R and $\Delta_{\rm xl}$, respectively. It can be understood from Fig. 4(a) that for $g_R < \kappa$, the squeezing is either zero or minimum. This is due to a vanishingly small value of K for $g_R < \kappa$. It is also clear from Fig. 4(a) that the maximum negative value of variance (maximum squeezing) is obtained for $\kappa = 0.7\Omega_R$ with $g_R \approx 1.5\Omega_R$ due to the increased value of K in the strong-coupling regime together with enhanced exciton coherence. Therefore, the optimum values of all concerned relevant parameters for achieving the maximum squeezing are found to be $\Omega_R = 25\ \mu$eV, $\Delta_{\rm xl} = -1.5\Omega_R$, $\Delta_{\rm cl} = -0.3\sqrt{\Omega_R^2 + \Delta_{\rm xl}^2}$, $\kappa = 0.7\Omega_R$, and $g_R = 1.5\Omega_R$. Furthermore, it should be noted that with these optimzed set of parameters $\Omega_R = 25\ \mu$eV, $g_R = 1.5\Omega_R$, and $\kappa = 0.7\Omega_R$, we operate in the strong QD-cavity coupling regime ($g_R > \kappa, \gamma$) and a strong excitation regime ($\Omega_R > \gamma$) [48]. Figure 4(b) illustrates the evolution of exciton coherence where both the numerically (dashed blue and dotted black lines) and the analytically (dashed-dot red and solid cyan lines) calculated coherence as a function of $\Delta_{\rm xl}$ for various Ω_R's are compared. It should particularly be observed that the analytically calculated coherence matches well with the numerically calculated coherence only for larger $\Delta_{\rm xl}$ but differs appeciably for smaller $\Delta_{\rm xl}$. This is precisely due to the assumption that the two-level QD system stays in its ground state for deriving the expression of $\langle\sigma^-\rangle$, which is perfectly satisfied only for large detuned $\Delta_{\rm xl} \gg \Omega_R$ excitation. Nevertheless, the approximate analytical expression of $\langle\sigma^-\rangle$ along with constant K clarifies that how exactly squeezing effect emerges in the present QD-cavity system [see Eq. (6)].

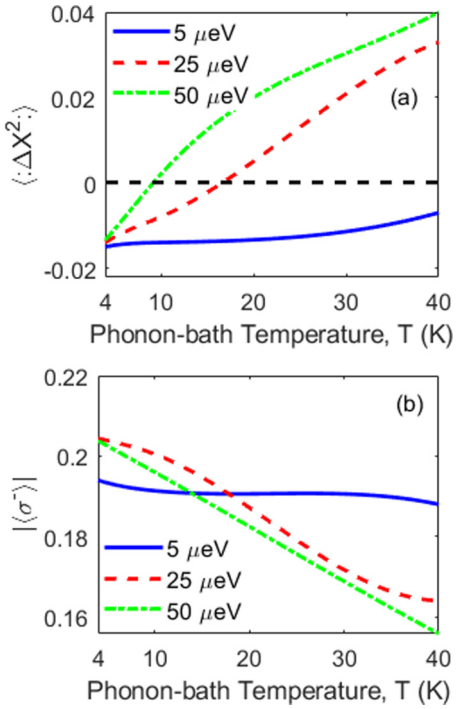

FIG. 5. Evolution of (a) variance $\langle : \Delta X^2 : \rangle$ and (b) cohrence $|\langle \sigma^- \rangle|$ as a function of phonon-bath temperature, T at the three different values of Rabi frequency, $\Omega_R = 5\ \mu$eV (solid blue line), $\Omega_R = 25\ \mu$eV (dashed red line), and $\Omega_R = 50\ \mu$eV (dashed-dot green line). The values of the other parameters are taken as $\Delta_{\rm xl} = -1.5\Omega_R$, $\Delta_{\rm cl} = -0.3\sqrt{\Omega_R^2 + \Delta_{\rm xl}^2}$, $g_R = 1.5\Omega_R$, and $\kappa = 0.7\Omega_R$. The horizontal dashed black line is a reference demarkation above which variance is positive and, hence, no squeezing.

B. Evolution of variance and exciton coherence as a function of phonon-bath temperature

So far, we have mainly investigated the squeezing of the cavity field by analyzing the variance for a fixed phonon-bath temperature $T = 4$ K. Therefore, we now display in Fig. 5(a), the evolution of variance for a quite wider range of phonon-bath temperature, ranging from 4 to 40 K for three different Ω_R's. It can clearly be seen that squeezing persits only up to $T = 8$ K for $\Omega_R = 50\ \mu$eV, whereas it can extend up to $T = 14$ and $T = 40$ K for $\Omega_R = 25$ and $\Omega_R = 5\ \mu$eV, respectively. Therefore, the squeezing effect is quite supressesed within a very short range of temperature for $\Omega_R = 50\ \mu$eV. It should be noted that the magnitude of phonon-induced incoherent rates $\Gamma_{\rm ph}^{\sigma^+}$, $\Gamma_{\rm ph}^{\sigma^-}$, $\Gamma_{\rm ph}^{a^\dagger\sigma^-}$, and $\Gamma_{\rm ph}^{\sigma^+ a}$ are squarely proportional to the Ω_R and g_R [see Eq. (3)]. Therefore, phonon-induced incoherent processes significantly supress the exciton coherence especially for larger values of Ω_R, resulting in the diminishing of squeezing within a shorter range of temperatureas seen for $\Omega_R = 50\ \mu$eV. We further illustrate this in Fig. 5(b) by showing the evolution of coherence $\langle \sigma^- \rangle$ as a function of temperature T for the same three Ω_R's as shown in Fig. 5(a). It can be observed that the decrement of $\langle \sigma^- \rangle$ increases with Ω_R as evident from slowly varying $\langle \sigma^- \rangle$ for $\Omega_R = 5\ \mu$eV as compared to $\Omega_R = 25$ and $\Omega_R = 50\ \mu$eV. Although, still coherence has a finite value even at $T = 40$ K for any chosen Ω_R, however, it does not seem to be sufficient for the realization of squeezing. A sufficient value of coherence $\langle \sigma^- \rangle$ is required below which the squeezing of cavity field does not persist as can be understood from Figs. 5(a) and 5(b).

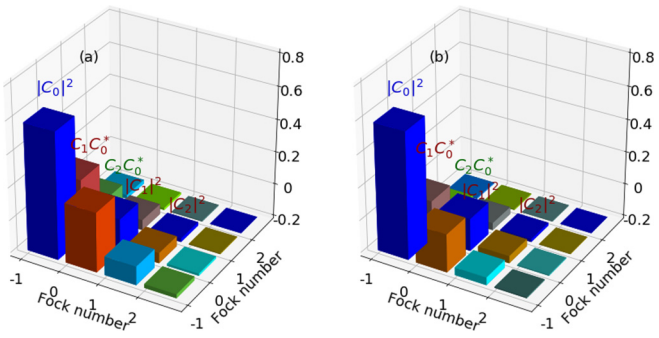

FIG. 6. Histogram of density-matrix elements of the cavity mode. (a) Phonon-bath temperature $T = 4$ K and (b) phonon-bath temperature $T = 40$ K. The values of the other parameters are taken as $\Omega_R = 25\ \mu$eV, $\Delta_{\rm xl} = -1.5\Omega_R$, $\Delta_{\rm cl} = -0.3\sqrt{\Omega_R^2 + \Delta_{\rm xl}^2}$, $g_R = 1.5\Omega_R$, and $\kappa = 0.7\Omega_R$.

C. Coherence between the Fock states of the cavity mode

Figure 6 displays the histogram of the population of different Fock states of the cavity mode and coherence between them. They are calculated numerically by tracing out the QD degrees of freedom using the quantum optics toolbox in PYTHON (QuTiP) [47]. The steady state of the cavity mode can be written as $|\psi\rangle = \sum_{n=0}^{n=2} C_n |n\rangle$. Here, we consider only up to two-photon Fock states since higher Fock states are not occupied at all as can be observed from Fig. 6 itself. The density-matrix operator of cavity mode is given as $\rho_{\rm cav} = |\psi\rangle\langle\psi| = [|C_0|^2|0\rangle\langle 0| + |C_1|^2|1\rangle\langle 1| + |C_2|^2|2\rangle\langle 2| + \{C_1C_0^*|1\rangle\langle 0| + C_2C_1^*|2\rangle\langle 1| + C_2C_0^*|2\rangle\langle 0| + \text{H.c.}\}]$ where density-matrix elements $|C_0|^2$, $|C_1|^2$, and $|C_2|^2$ represent the occupation probabilty of zero-, one-, and two-photon Fock states, respectively, whereas $C_1C_0^*$, $C_2C_1^*$, and $C_2C_0^*$ represent the cohrence among zero-, one-photon, one-, two-photon, zero-, and two-photon Fock states, respectively. The diagonal blue bars represent the occupation probabilities of the Fock states, whereas off-diagonal bars represent the coherence between the relevant Fock states.

The signifiance of coherence between Fock states becomes clear and evident when we deduce the expressions for the expectation values of annihilation operator a and a^2 using $\langle O \rangle = \text{Tr}(O\rho_{\rm cav})$. The expectation value of a and a^2 are given as $\langle a \rangle = C_1C_0^* + C_2C_1^*$ and $\langle a^2 \rangle = C_2C_0^*$, respectively. From these expressions, it is quite easy to comprehend that if there is no coherence ($C_1C_0^* = C_2C_1^* = C_2C_0^* = 0$) then the values of $\langle a \rangle$ and $\langle a^2 \rangle$ will vanish, and variance can never be negative, i.e., there will be no squeezing of the cavity field [see Eq. (4)]. It can be observed from Fig. 6(a) that each $C_1C_0^*$, $C_2C_1^*$, and $C_2C_0^*$ has a finite value, resulting in the finite values of $\langle a \rangle$ and $\langle a^2 \rangle$. Both $\langle a \rangle$ and $\langle a^2 \rangle$ depend on $\langle \sigma^- \rangle$ [see Eqs. (7) and (8)]. Therefore, it becomes clear that the exciton coherence $\langle \sigma^- \rangle$

results in the creation of coherence among zero-, one-photon, one-, two-photon, zero-, and two-photon Fock states of the cavity mode. In Fig. 6(b), we show the histogram of the density-matrix elements with the same set of parameters as employed in Fig. 6(a) but at $T = 40$ K. It can be observed that $C_1C_0^*$, $C_2C_1^*$, and $C_2C_0^*$ decrease appreciably. This occurs due to the substantial reduction of the exciton coherence [see Fig. 5(b)], and, therefore, no squeezing persists at $T = 40$ K.

IV. CONCLUSIONS

We have investigated a coherently driven quantum dot strongly coupled to a single-mode pillar microcavity by employing an effective polaron master equation theory for accurately incorporating the effects of exciton-phonon coupling. The detailed numerical investigation is carried out to optimize the concerned parameters for obtaining the maximal squeezing of the cavity field. We have derived an analytical expression of the normally ordered varaince for clarifying the connection between squeezing and exciton coherence. We have shown that the squeezing origiates from the buildup of maximal exciton coherence which results in the creation of appreciable coherence among zero-, one-photon, zero-, and two-photon Fock states of the cavity mode. We have also investigated the effect of temperature-dependent exciton-phonon coupling. It is shown that the squeezing decreases with phonon-bath temperature, and it does not persist beyond 14 K at the optimum Rabi frequency $\Omega_R = 25$ μeV.

ACKNOWLEDGMENTS

This work was partially supported by a Dr. D. S. Kothari Postdoctoral Research Fellowship, University Grant Commission, India, through Grant No. F.4-2/2006 (BSR)/PH/15-16/0077. P.K. would like to thank Professor A. K. Sarma for the useful discussions.

APPENDIX: DERIVATION OF THE VARIANCE [EQ. (6)]

We derive an analytical expression of the variance of cavity field [Eq. (6)] by following Ref. [24]. However, it is to be noted that in Ref. [24] the cavity mode is excited by the laser light. Whereas, we consider a quantum dot which is directly excited by the laser light. The time evolution of the expectation value of an operator, O is computed as $\frac{d\langle O\rangle}{dt} = \mathrm{Tr}(O\frac{d\rho}{dt})$. We derive the following equations for the expectation values of relevant operators using Eq. (1) given in the main body of the paper,

$$\frac{d\langle a\rangle}{dt} = i[\tilde{\omega}_c\langle a\rangle - g_R\langle\sigma^-\rangle], \tag{A1}$$

$$\frac{d\langle\sigma^-\rangle}{dt} = i\left[\tilde{\omega}_a\langle\sigma^-\rangle + g_R\langle a\sigma_z\rangle + \frac{\Omega_R}{2}\langle\sigma_z\rangle\right], \tag{A2}$$

$$\frac{d\langle a^2\rangle}{dt} = 2i[\tilde{\omega}_c\langle a^2\rangle - g_R\langle a\sigma^-\rangle], \tag{A3}$$

$$\frac{d\langle a\sigma^-\rangle}{dt} = i\left[(\tilde{\omega}_a + \tilde{\omega}_c)\langle a\sigma^-\rangle + g_R\langle a^2\sigma_z\rangle + \frac{\Omega_R}{2}\langle a\sigma_z\rangle\right]. \tag{A4}$$

For simplicity, we neglect the phonon-induced incoherent rates, $\Gamma_{\mathrm{ph}}^{\sigma^+}$, $\Gamma_{\mathrm{ph}}^{\sigma^-}$, $\Gamma_{\mathrm{ph}}^{a^\dagger\sigma^-}$, and $\Gamma_{\mathrm{ph}}^{\sigma^+a}$ in the above equations. The complex detunings are defined as $\tilde{\omega}_c = (-\Delta_{\mathrm{cl}} + i\frac{\kappa}{2})$, $\tilde{\omega}_a = (-\Delta_{\mathrm{xl}} + i\frac{\gamma}{2})$. The population inversion $\langle\sigma_z\rangle$ is defined as $\langle\sigma_z\rangle = [\sigma^+\sigma^- - \sigma^-\sigma^+]$. We assume that the population in exciton state $|e\rangle$ is negligible under large-detuned driving of QD, $\Delta_{xl} \gg \Omega_R$. In this limit $\langle\sigma_z\rangle \approx -1$, $\langle a\sigma_z\rangle \approx -\langle a\rangle$, $\langle a^2\sigma_z\rangle \approx -\langle a^2\rangle$, and from Eqs. (A1)–(A4), the steady-state values of $\langle a\rangle$, $\langle a^2\rangle$, and $\langle\sigma^-\rangle$ read as

$$\langle a\rangle = \frac{g_R\Omega_R}{2\left[\tilde{\omega}_a\tilde{\omega}_c - g_R^2\right]}, \tag{A5}$$

$$\langle a^2\rangle = \frac{g_R^2\Omega_R^2}{4\left[\tilde{\omega}_a\tilde{\omega}_c - g_R^2\right]\left[\tilde{\omega}_c(\tilde{\omega}_a + \tilde{\omega}_c) - g_R^2\right]}, \tag{A6}$$

$$\langle\sigma^-\rangle = \frac{\Omega_R\tilde{\omega}_c}{2\left[\tilde{\omega}_a\tilde{\omega}_c - g_R^2\right]}. \tag{A7}$$

From Eqs. (A5) and (A6), the fluctuation of the cavity field read as

$$\Delta a^2 = \frac{g_R^2\Omega_R^2\tilde{\omega}_c^2}{4\left[\tilde{\omega}_a\tilde{\omega}_c - g_R^2\right]^2\left[\tilde{\omega}_c(\tilde{\omega}_a + \tilde{\omega}_c) - g_R^2\right]}. \tag{A8}$$

The complex detunings of the dressed states are defined as

$$\tilde{\omega}_{n\pm} = (n-1)\tilde{\omega}_c + \tfrac{1}{2}(\tilde{\omega}_a + \tilde{\omega}_c) \mp \tfrac{1}{2}\sqrt{4ng_R^2 + (\tilde{\omega}_c - \tilde{\omega}_a)^2}, \tag{A9}$$

which allow us to write $\langle\sigma^-\rangle$, $\langle a\rangle$, $\langle a^2\rangle$, and Δa^2 as

$$\langle\sigma^-\rangle = \frac{\Omega_R\tilde{\omega}_c}{2(\tilde{\omega}_{1+}\tilde{\omega}_{1-})}, \tag{A10}$$

$$\langle a\rangle = \frac{\Omega_R g_R}{2(\tilde{\omega}_{1+}\tilde{\omega}_{1-})}, \tag{A11}$$

$$\langle a^2\rangle = \frac{\Omega_R}{\tilde{\omega}_c}K\langle\sigma^-\rangle, \tag{A12}$$

$$\Delta a^2 = -K\langle\sigma^-\rangle^2, \tag{A13}$$

where the constant K is given by

$$K = \frac{2g_R^2}{(\tilde{\omega}_{2+}\tilde{\omega}_{2-})}, \tag{A14}$$

The variance of the cavity field [Eq. (6)] reads as

$$\langle : \Delta X^2 : \rangle \approx -\tfrac{1}{2}\mathrm{Re}(K\langle\sigma^-\rangle^2). \tag{A15}$$

[1] A. Nielsen and I. L. Chuang, *Quantum Computation and Quantum Information* (Cambridge University Press, Cambridge, UK, 2000).

[2] E. Andersson and P. Öhberg, *Quantum Information and Coherence (Scottish Graduate Series* (Springer, Berlin, 2014) .

[3] L. Mandel and E. Wolf, *Optical Coherence and Quantum Optics* (Cambridge University Press, Cambridge, UK, 2013).

[4] P. Giorda and M. Allegra, Coherence in quantum estimation, J. Phys. A: Math. Theor. **51**, 025302 (2017).

[5] B. S. Ham, Deterministic control of photonic de Broglie waves using coherence optics, Sci. Rep. **10**, 12899 (2020).

[6] C. Zhang, T. R. Bromley, Y.-F. Huang, H. Cao, W.-M. Lv, B.-H. Liu, C.-F. Li, G.-C. Guo, M. Cianciaruso, and G. Adesso, Demonstrating quantum coherence and metrology that is resilient to transversal noise, Phys. Rev. Lett. **123**, 180504 (2019).

[7] S. F. Huelga and M. B. Plenio, Vibrations, quanta and biology, Contemp. Phys. **54**, 181 (2013).

[8] S. Lloyd, Quantum coherence in biological systems, J. Phys.: Conf. Ser. **302**, 012037 (2011)

[9] M. Lostaglio, K. Korzekwa, D. Jennings, and T. Rudolph, Quantum Coherence, Time-Translation Symmetry, and Thermodynamics, Phys. Rev. X **5**, 021001 (2015).

[10] P. Rebentrost, M. Mohseni, and A. Aspuru-Guzik, Role of quantum coherence and environmental fluctuations in chromophoric energy transport, J. Phys. Chem. B **113**, 9942 (2009).

[11] X. Xu, B. Sun, P. R. Berman, D. G. Steel, A. S. Bracker, D. Gammon, and L. J. Sham, Coherent population trapping of an electron spin in a single negatively charged quantum dot, Nat. Phys. **4**, 692 (2008).

[12] S. G. Carter, S. C. Badescu, A. S. Bracker, M. K. Yakes, K. X. Tran, J. Q. Grim, and D. Gammon, Coherent Population Trapping Combined with Cycling Transitions for Quantum Dot Hole Spins Using Triplet Trion States, Phys. Rev. Lett. **126**, 107401 (2021).

[13] S. Das, P. Liu, B. Grémaud, and M. Mukherjee, Magnetic coherent population trapping in a single ion, Phys. Rev. A **97**, 033838 (2018).

[14] S. E. Harris, Electromagnetically induced transparency, Phys. Today **50**(7), 36 (1997).

[15] M. Fleischhauer, Electromagnetically induced transparency and coherent-state preparation in optically thick media, Opt. Express **4**, 107 (1999).

[16] H. Q. Fan, K. H. Kagalwala, S. V. Polyakov, A. L. Migdall, and E. A. Goldschmidt, Electromagnetically induced transparency in inhomogeneously broadened solid media, Phys. Rev. A **99**, 053821 (2019).

[17] Y. Zhu, J. Saldana, L. Wen, and Y. Wu, Steady-state population inversion by multiphoton electromagnetically induced transparency, J. Opt. Soc. Am. B **21**, 806 (2004).

[18] M. Marthaler, Y. Utsumi, D. S. Golubev, A. Shnirman, and Gerd Schön, Lasing without Inversion in Circuit Quantum Electrodynamics, Phys. Rev. Lett. **107**, 093901 (2011).

[19] P. Grünwald and W. Vogel, Optimal Squeezing in Resonance Fluorescence Via Atomic-State Purification, Phys. Rev. Lett. **109**, 013601 (2012).

[20] N. Német and S. Parkins, Enhanced optical squeezing from a degenerate parametric amplifier via time-delayed coherent feedback, Phys. Rev. A **94**, 023809 (2016).

[21] H. H. Adamyan, J. A. Bergou, N. T. Gevorgyan, and G. Y. Kryuchkyan, Strong squeezing in periodically modulated optical parametric oscillators, Phys. Rev. A **92**, 053818 (2015).

[22] C. F. McCormick, A. M. Marino, V. Boyer, and P. D. Lett, Strong low-frequency quantum correlations from a four-wave-mixing amplifier, Phys. Rev. A **78**, 043816 (2008).

[23] Q. Glorieux, R. Dubessy, S. Guibal, L. Guidoni, J.-P. Likforman, T. Coudreau, and E. Arimondo, Double- microscopic model for entangled light generation by four-wave mixing, Phys. Rev. A **82**, 033819 (2010).

[24] A. Ourjoumtsev, A. Kubanek, M. Koch, C. Sames, P. Pinkse, G. Rempe, and K. Murr, Observation of squeezed light from one atom excited with two photons, Nature (London) **474**, 623 (2011).

[25] K. Qu and G. S. Agarwal, Generating quadrature squeezed light with dissipative optomechanical coupling, Phys. Rev. A **91**, 063815 (2015).

[26] V. Peano, H. G. L. Schwefel, Ch. Marquardt, and F. Marquardt, Intracavity Squeezing Can Enhance Quantum-Limited Optomechanical Position Detection Through Deamplification, Phys. Rev. Lett. **115**, 243603 (2015).

[27] C. Gross Estève, A. Weller, S. Giovanazzi, and M. K. Oberthaler, Squeezing and entanglement in a Bose-Einstein condensate, Nature (London) **455**, 1216 (2008).

[28] V. Giovannetti, S. Lloyd, and L. Maccone, Advances in quantum metrology, Nat. Photon. **5**, 222 (2011).

[29] J. Aasi *et al.*, Enhanced sensitivity of the LIGO gravitational wave detector by using squeezed states of light, Nat. Photon. **7**, 613 (2013).

[30] Y. Zhao, N. Aritomi, E. Capocasa, M. Leonardi, M. Eisenmann, Y. Guo, E. Polini, A. Tomura, K. Arai, Y. Aso, Y.-C. Huang, R.-K. Lee, H. Lück, O. Miyakawa, P. Prat, A. Shoda, Matteo. Tacca, R. Takahashi, H. Vahlbruch, M. Vardaro, C.-M. Wu, M. Barsuglia, and R. Flaminio, Frequency-Dependent Squeezed Vacuum Source for Broadband Quantum Noise Reduction in Advanced Gravitational-Wave Detectors, Phys. Rev. Lett. **124**, 171101 (2020).

[31] U. L. Andersen, T. Gehring, C. Marquardt, and G. Leuchs, 30 years of squeezed light generation, Phys. Scr. **91**, 053001 (2016).

[32] D. D. B. Rao, S. Yang, and J. Wrachtrup, Generation of entangled photon strings using NV centers in diamond, Phys. Rev. B **92**, 081301(R) (2015).

[33] P. Kumar and A. G. Vedeshwar, Phonon-assisted control of the single-photon spectral characteristics in a semiconductor quantum dot using a single laser pulse, Phys. Rev. A **96**, 033808 (2017).

[34] S. Tamariz, G. Callsen, J. Stachurski, K. Shojiki, R. Butté, and N. Grandjean, Toward bright and pure single photon emitters at 300 K based on GaN quantum dots on silicon, ACS Photon. **7**, 1515 (2020).

[35] M. Zeeshan, N. Sherlekar, A. Ahmadi, R. L. Williams, and M. E. Reimer, Proposed Scheme to Generate Bright Entangled Photon Pairs by Application of a Quadrupole Field to a Single Quantum Dot, Phys. Rev. Lett. **122**, 227401 (2019).

[36] W. Song, W. Yang, J. AN, and M. Feng, Dissipation-assisted spin squeezing of nitrogen-vacancy centers coupled to a rectangular hollow metallic waveguide, Opt. Express **25**, 19227 (2017).

[37] P. Kumar and A. G. Vedeshwar, Generation of frequency-tunable squeezed single photons from a single quantum dot, J. Opt. Soc. Am. B **35**, 3035 (2018).

[38] C. H. H. Schulte, J. Hansom, A. E. Jones, C. Matthiesen, C. L. Gall, and M. Atatüre, Quadrature squeezed photons from a two-level system, Nature (London) **525**, 222 (2015).

[39] J. I.-Smith, A. Nazir, and D. P. S. McCutcheon, Vibrational enhancement of quadrature squeezing and phase sensitivity in resonance fluorescence, Nat. Commun. **10**, 3034 (2019).

[40] P. Kumar and A. G. Vedeshwar, Cavity-assisted enhanced and dephasing-immune squeezing in the resonance fluorescence of a single quantum dot, Phys. Rev. A **102**, 043715 (2020).

[41] A. J. Ramsay, A. V. Gopal, E. M. Gauger, A. Nazir, B. W. Lovett, A. M. Fox, and M. S. Skolnick, Damping of Exciton Rabi Rotations by Acoustic Phonons in Optically Excited InGaAs/GaAs Quantum Dots, Phys. Rev. Lett. **104**, 017402 (2010).

[42] A. J. Ramsay, T. M. Godden, S. J. Boyle, E. M. Gauger, A. Nazir, B. W. Lovett, A. M. Fox, and M. S. Skolnick, Phonon-Induced Rabi-Frequency Renormalization of Optically Driven Single InGaAs/GaAs Quantum Dots, Phys. Rev. Lett. **105**, 177402 (2010).

[43] D. P. S. McCutcheon and A. Nazir, Model of the Optical Emission of a Driven Semiconductor Quantum Dot: Phonon-Enhanced Coherent Scattering and Off-Resonant Sideband Narrowing, Phys. Rev. Lett. **110**, 217401 (2013).

[44] N. Makri and D. E. Makarov, Tensor propagator for iterative quantum time evolution of reduced density matrices. I. Theory, J. Chem. Phys. **102**, 4600 (1995).

[45] C. Roy and S. Hughes, Influence of Electron–Acoustic-Phonon Scattering on Intensity Power Broadening in a Coherently Driven Quantum-Dot–Cavity System, Phys. Rev. X **1**, 021009 (2011).

[46] S. Hughes and H. J. Carmichael, Phonon-mediated population inversion in a semiconductor quantum-dot cavity system, New J. Phys. **15**, 053039 (2013).

[47] J. R. Johansson, P. D. Nation, and F. Nori, QuTiP: An open-source python framework for the dynamics of open quantum systems, Comput. Phys. Commun. **183**, 1760 (2012).

[48] H. Freedhoff and T. Quang, Steady-state resonance fluorescence spectrum of a two-level atom in a cavity, J. Opt. Soc. Am. B **10**, 1337 (1993).